Gramicidin Conducting Dimers in Lipid Bilayers Are Stabilized by Single-File Ionic Flux along Them

Lucia Becucci, Alessandra Santucci, and Rolando Guidelli*

Department of Chemistry, Florence University, via della Lastruccia 3, 50019 Sesto Fiorentino (Firenze), Italy

Received: March 14, 2007; In Final Form: June 18, 2007

Gramicidin D was incorporated in a biomimetic membrane consisting of a lipid bilayer tethered to a mercury electrode via a hydrophilic spacer, and its behavior was investigated in aqueous 0.1 M KCl by potential-step chronocoulometry and electrochemical impedance spectroscopy. The impedance spectra, recorded from 0.1 to 1×10^5 Hz over a potential range of 0.7 V, were fitted to a series of *RC* meshes, which were related to the different substructural elements of the biomimetic membrane. These impedance spectra were compared with those obtained by incorporating valinomycin, under otherwise identical conditions. The potential dependence of the stationary currents reported on bilayer lipid membranes by Bamberg and Läuger (Bamberg, E.; Läuger, P. *J. Membrane Biol.* **1973**, *11*, 177−194) as well as those extracted from potential-step chronocoulometric measurements was interpreted by relating the increase in gramicidin dimerization to a progressive increase in single-file K^+ flux along the dimeric channels. An analogous approach was adopted in explaining the difference between the impedance spectra obtained with gramicidin D and those obtained with valinomycin. It is concluded that gramicidin has a low tendency to form dimers in the absence of ionic flux.

Introduction

Gramicidin is a neutral linear hydrophobic pentadecapeptide with an L,D-alternating sequence. The natural mixture of gramicidin, produced by *Bacillus brevis*, consists of about 80% of gramicidin A, 5% of B, and 15% of C, with tryptophan (Trp), phenylalanine (Phe), and tyrosine (Tyr) in position 11, respectively. In organic solvents, gramicidin is present in a conformation equilibrium between different monomeric and dimeric, double-stranded (ds) species.[1−5] Ds-dimeric species predominate in nonpolar solvents, and monomeric species dominate in polar ones.[2,5,6] Upon incorporating gramicidin in a lipid bilayer from a polar solvent, it adopts a single-stranded $\beta^{6.3}_{3.3}$-helical conformation.[7−12] It is now well accepted that this conformation is responsible for ion-channel formation across the lipid bilayer.[13−17] The ion channels consist of N-terminus-to-N-terminus dimers, probably via the formation of six intramolecular hydrogen bonds.[13,14,18] In fact, the hydrocarbon tail portion of a bilayer, whose length ranges from 30 to 40 Å, can only be spanned by two aligned gramicidin molecules, which form a channel about 25−30 Å long.[18] If gramicidin is incorporated in a lipid bilayer from nonpolar solvents, the ds-dimeric conformation initially predominates. This conformation, which may span the whole lipid bilayer with a nonchannel structure, is in a metastable state that slowly dissociates, refolding into the $\beta^{6.3}_{3.3}$-helical conformation.[7−12] Progressive substitution of the four Trp residues, located at the C-terminus end, by Phe residues tends to shift the conformational equilibrium from channel-forming monomers to nonconducting ds-dimers in DOPC bilayers.[19−21] In the monosubstituted analogues of gramicidin A, the destabilization of the monomeric structure in favor of the ds-dimeric one is greater for Trp substitution in the 9 and 13 positions, while it is definitely smaller in the 11 and 15 positions.[21] It has been suggested that hydrogen bond formation between Trp residues and the polar head region of the bilayer may be the driving force for the unwinding of ds-dimers in the membrane.[9,22,23] Lipid spin label measurements indicate that the N-terminus is located deep in the membrane, while the C-terminus is not.[17] These findings, besides pointing to the N-terminus-to-N-terminus helical dimer as the major conformation of the gramicidin channel, support the location of the Trp residues in the polar head region of the membranes due to their H-bonding capability and favorable electrostatic interactions. A gramicidin derivative negatively charged at the C-terminus does not form channels when added to only one side of a bilayer lipid membrane (BLM), while it forms them when added to both sides.[16] Conversely, gramicidin forms channels even if added to one side of the BLM. This indicates that gramicidin, as opposed to its negatively charged analogue, can easily cross the membrane. Moreover, the two halves of the gramicidin channel can combine via the N-termini only if they are present on opposite sides of the bilayer, with the C-termini embedded in the corresponding polar head regions. The strongly hydrophobic nature and the poor water solubility of gramicidin make it difficult to obtain reproducible values of conductivity of lipid bilayers with given amounts of gramicidin added to the aqueous solutions.[16] Consequently, the partition coefficient of gramicidin between a lipid bilayer and water is not known. A partition coefficient of 4.8×10^{-3} cm was reported for its negatively charged analogue, *O*-pyromellityl-gramicidin,[16] which, however, has a much higher solubility in water.

Potential steps from a zero transmembrane potential, $\phi_2 = 0$, to progressively increasing ϕ_2 values yield current transients that start from a small initial value, I_0, and relax monoexponentially to a final stationary value, I_∞.[24] While I_0 shows a modest linear increase with ϕ_2, denoting an Ohmic behavior, I_∞ increases with ϕ_2 more than linearly, showing a roughly

* To whom correspondence should be addressed. Phone: +39 055 457 3097. Fax: +39 055 457 3385. E-mail: guidelli@unifi.it.

10.1021/jp072051p CCC: $37.00
Published on Web 08/02/2007

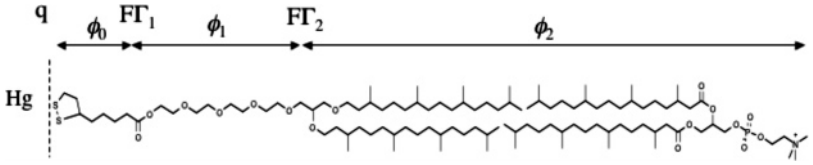

Figure 1. Schematic picture of the different substructures of a tBLM with the primary structure of the DPTL thiolipid in contact with that of a diphytanoylphosphatidylcholine molecule. The figure shows the electric potential differences across the different substructures and the proposed location of the different charges.

quadratic dependence upon ϕ_2.[25] The notable increase in the I_∞/I_0 ratio with an increase in ϕ_2 clearly reflects an increase in the number of conducting channels following the potential step. The monoexponential increase of the current with time for each potential step was satisfactorily explained by the bimolecular kinetics of dimer formation from gramicidin monomers. However, the notable increase in the association rate constant and in the corresponding equilibrium constant for dimer formation with an increase in ϕ_2 (the dissociation rate constant is practically independent of ϕ_2) has not found a satisfactory explanation. Bamberg and Läuger[24] tentatively explained this increase with a voltage-induced decrease in the membrane thickness, which favors a more precise matching of the two monomers. Subsequently, Bamberg and Benz[25] showed that the increase in the association rate constant with ϕ_2 does not correlate with the thickness change of the lipid membrane and suggested a more direct effect of the electric field, based on a proposal by Urry.[14] According to the latter author, gramicidin may exist in two kinetically interconvertible and energetically similar conformations, one conducting and the other nonconducting; the conducting one is the $\beta^{6.3}_{3.3}$-helical conformation originally proposed by Urry himself[13] and nowadays universally accepted as being responsible for the formation of the N-terminus-to-N-terminus conducting dimer. While Urry's nonconducting conformation is nonpolar, the $\beta^{6.3}_{3.3}$-conformation has a dipole moment of more that 0.5 Debye per L,D-dipeptide unit.[14] According to Bamberg and Benz,[25] the increase in the association rate constant with an increase in ϕ_2 can be tentatively explained by a gradual shift from the nonpolar, nonconducting conformation to the polar, conducting one. These authors also observed that "a field change that is energetically favorable for the active form of the monomer in one-half of the bilayer is unfavorable in the other half". Nonetheless, in their treatment, they ignored that the number densities of the two gramicidin monomers forming the channel have an opposite dependence upon the transmembrane potential, in view of the opposite orientation of their dipoles with respect to the applied electric field. If this feature is accounted for, it is intuitive that the maximum stability of the dimeric channel is attained at zero transmembrane potential; a potential shift in any of the two directions will favor one monomeric orientation at the expense of the other, destabilizing the dimer. The reason for the increase in the stability of the conducting dimeric channel with an increase in field strength must, therefore, find a different explanation.

This Letter aims at providing evidence that the stability of the dimeric channels increases with the ionic flux along them. In other words, the more rapid the single-file motion of ions along the gramicidin channels is, the more it prevents their dissociation. In fact, when the time elapsed between the passage of two consecutive cations through the junction between the two monomers forming the conducting dimer starts to become comparable with, and ultimately shorter than, the time required for the mismatch between the two monomers with dimer dissociation, the latter event is expected to become less probable. In this respect, the potential dependence of the equilibrium constant for dimer formation assumes a dynamic character. Measurements were carried out by incorporating gramicidin in a mercury-supported biomimetic membrane. This was obtained by tethering to a mercury electrode a "thiolipid" consisting of a tetraethyleneoxy (TEO) hydrophilic chain terminated at one end with a disulfide group, for anchoring to the mercury surface, and covalently linked at the other end to two phytanyl chains mimicking the hydrocarbon tails of a phospholipid.[26−30] By self-assembling a diphytanoylphosphatidylcholine monolayer on top of the thiolipid monolayer, a lipid bilayer is obtained, which is interposed between the TEO hydrophilic "spacer" and a 0.1 M KCl aqueous electrolyte. The primary structure of a thiolipid molecule anchored to a metal surface and of a diphytanoylphosphatidylcholine molecule in contact with it is shown in Figure 1. The behavior of the resulting tethered bilayer lipid membrane (tBLM) was investigated by electrochemical impedance spectroscopy and potential-step chronocoulometry.

Experimental Methods

The water used was obtained from water produced by an inverted osmosis unit, upon distilling it once and then distilling the water so-obtained from alkaline permanganate. Merck suprapur KCl was baked at 500 °C before use to remove any organic impurities. Diphytanoylphosphatidylcholine (DphyPC) was purchased from Avanti Polar Lipids (Birmingham, AL). The advantage of diphytanoyl lipids over unbranched lipids of equal chain length is that they have a gel-to-liquid-crystalline-state transition temperature much lower than room temperature without having double bonds, which makes lipids oxidizable by air. Gramicidin D was purchased from Sigma and used without further purification. The 2,3-di-*O*-phytanyl-*sn*-glycerol-1-tetraethylene-glycol-D,L-α-lipoic acid ester lipid (DPTL) was provided by Professor Adrian Schwan (Department of Chemistry, University of Guelph, Canada). The other chemicals and solvents were commercially available and used as received.

DphyPC solutions were prepared by diluting a proper amount of stock solution of this phospholipid with pentane. Solutions of 0.2 mg/mL DPTL in ethanol were prepared from a 2 mg/mL solution of DPTL in ethanol. Stock solutions of this thiolipid were stored at −18 °C. Stock solutions of 3.6×10^{-4} M gramicidin were prepared in ethanol and stored at +4 °C.

All measurements were carried out in aqueous 0.1 M KCl. A homemade hanging mercury drop electrode (HMDE) described elsewhere,[31] 8.4×10^{-2} cm in radius, was employed. Use was made of a homemade glass capillary with a finely tapered tip, about 1 mm in outer diameter and 0.2 mm in inner diameter. Capillary and mercury reservoirs were thermostated at 25 ± 0.1 °C by the use of a water-jacketed box to avoid any changes in drop area due to a change in temperature. One glass electrolysis cell containing the aqueous solution and a small glass vessel containing the ethanol solution of the thiolipid were placed on a movable support inside of the box.[32] The HMDE and the support were moved vertically and horizontally,

respectively, by means of two oleodynamic systems that ensured the complete absence of vibrations.

AC voltammetry, potential-step chronocoulometry, and electrochemical impedance spectroscopy measurements were carried out with an Autolab instrument PGSTAT 12 (Echo Chemie) supplied with FRA2 module for impedance measurements, a SCAN-GEN scan generator, and GPES 4.9 software. Potentials were measured versus an Ag|AgCl electrode immersed in the KCl working solution but are referred to a saturated calomel electrode (SCE).

Monolayers of DPTL were self-assembled on the HMDE by keeping the mercury drop immersed in the small vessel containing the thiolipid solution for 20 min. In the meantime, a pentane solution of DphyPC was spread on the surface of the aqueous solution in the glass cell in an amount corresponding to five to six phospholipid monolayers, and the pentane was allowed to evaporate. Using the oleodynamic system, the DPTL-coated HMDE was then extracted from the vessel, washed with ethanol to remove the excess of adsorbed thiolipid, and kept in a N_2 atmosphere for the time strictly necessary to allow the solvent to evaporate. Immediately afterward, the electrolysis cell containing the aqueous solution on whose surface DphyPC had been previously spread was brought below the HMDE, and the latter was lowered so as to immerse it into the aqueous solution across the phospholipid film; this procedure caused a DphyPC monolayer to self-assemble on top of the DPTL monolayer, giving rise to a lipid bilayer interposed between the hydrophilic moiety of the thiolipid and the aqueous solution. The applied potential was then repeatedly scanned over a potential range from -0.200 to -1.200 V while continuously monitoring the curve of the quadrature component, Y'', of the electrode admittance at 75 Hz against the applied potential, E, until a stable Y'' versus E curve was attained. The minimum Y''/ω value for the resulting DPTL|DphyPC-coated mercury, where ω is the angular frequency, ranged from 0.55 to 0.65 μF cm^{-2} and was therefore close to the capacity, $\sim$0.8 μF cm^{-2}, of a solvent-free black lipid membrane. Gramicidin was incorporated in this tBLM by simply adding its stock solution to the electrolysis cell in an amount corresponding to 1.0×10^{-7} M. The solution was then stirred for a few minutes while keeping the electrode at an applied potential of -0.500 V.

Results

In the absence of ionic flux, the zero potential difference across the lipid bilayer moiety of the tBLM (namely, the zero transmembrane potential ϕ_2), as estimated from independent measurements, was attained at an applied potential of about -0.500 V/SCE;[33,34] moreover, in view of the values of the capacities of the three substructures composing the tBLM (see Figure 1), the fraction of the potential difference across the whole tBLM that was localized in the lipid bilayer moiety amounted to about 70%. Therefore, the transmembrane potential ϕ_2 depends upon the applied potential E according to the equation $\phi_2 = 0.7 \times (E + 0.500\ \text{V})$.

Figure 2 shows a number of charge versus time curves following a series of potential steps from a fixed initial potential of -0.200 V to progressively more negative final potentials, E_f, on a tBLM incorporating gramicidin from its 1.0×10^{-7} M solution in aqueous 0.1 M KCl. The electrode was kept at the initial potential of -0.200 V for 5 min before each potential step. During this rest time, potassium ions were almost completely expelled from the TEO moiety by electrostatic repulsion. The higher the negative potential step, the larger the amount of K^+ ions moved into the TEO moiety along the gramicidin channels. Ultimately, the TEO moiety was saturated with K^+ ions, and the charge attained a constant limiting value. The plateau of the charge versus time curves was attained at shorter times as E_f was made more negative. The height of the plateau amounted to about -45 μC cm^{-2}; it can be regarded as a measure of the maximum charge of potassium ions that can be accommodated in the hydrophilic TEO moiety. In fact, the flux of K^+ ions into the TEO moiety along the gramicidin channels, following a potential step, created a potential difference across the lipid bilayer moiety, positive toward the metal. At a constant final potential E_f, this potential difference was compensated for by an equal and opposite potential difference created by a flow of electrons to the metal surface along the external circuit; this gave rise to a negative contribution to the capacitive current, in addition to the capacitive current recorded in the absence of gramicidin. When the TEO moiety was completely saturated by the K^+ ions, this negative contribution attained a maximum limiting value, just as the corresponding charge. Before tending to the above limiting value, the curves of the charge Q against the time t exhibited an initial, roughly linear section, whose slope measured the "stationary current" that would be maintained if there were no limitation to K^+ diffusion on the metal side of the lipid bilayer moiety, as is the case with traditional BLMs. The fitting of the initial linear section of the Q versus t curves to a straight line was carried out over the maximum time range, ensuring a level of confidence of no less that 99.9%. The resulting slope is plotted against the transmembrane potential ϕ_2 in Figure 3 (solid triangles). For comparison, Figure 3 also shows the stationary current at a BLM in an aqueous solution of 1 M NaCl and 2×10^{-11} M gramicidin A (open squares), as reported in Figure 2 of ref 24. In the figure, the transmembrane potential was taken as negative on the side of the lipid bilayer toward which the K^+ ions moved. It is apparent that the stationary current increased with $|\phi_2|$ much more than linearly.

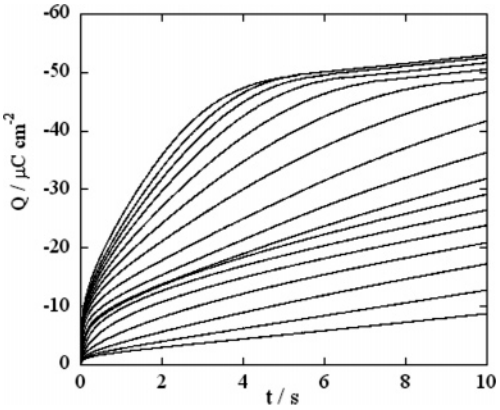

Figure 2. Charge versus time curves following potential steps from a fixed initial potential of -0.200 V to progressively more negative final potentials, E_f, varying from -0.525 to -0.925 V by -25 mV increments, at a tBLM incorporating gramicidin from its 1.0×10^{-7} M solution in aqueous 0.1 M KCl.

Impedance spectra of tBLMs incorporating gramicidin were recorded in aqueous 0.1 M KCl, upon varying the bias potential from -0.30 to -1.00 V by -25 mV steps and varying the frequency from 0.1 to 1×10^5 Hz at each potential. The presence of gramicidin increased both the in-phase and the quadrature components of the tBLM admittance. Figure 4 shows a plot of $\omega Z'$ versus $\omega Z''$ for a tBLM incorporating gramicidin from its 1.0×10^{-7} M solution in 0.1 M KCl, at a potential of -0.525 V; ω is the angular frequency, and Z' and Z'' are the in-phase and quadrature components of the impedance. Three partially

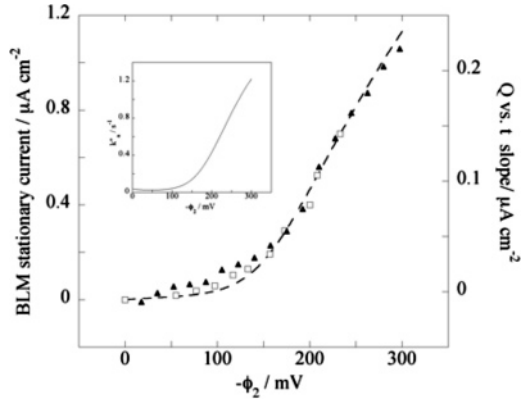

Figure 3. The solid triangles are values of the slope of the linear portion of the charge versus time curves in Figure 2, plotted against the transmembrane potential ϕ_2 estimated as described in the text. The open squares are values of the stationary current at a BLM incorporating gramicidin A from its 2×10^{-11} M solution in aqueous 1 M NaCl plotted against ϕ_2 (from Figure 2 in ref 24). The dashed curve was calculated as described in the text, just as the k_a'' versus ϕ_2 plot in the inset.

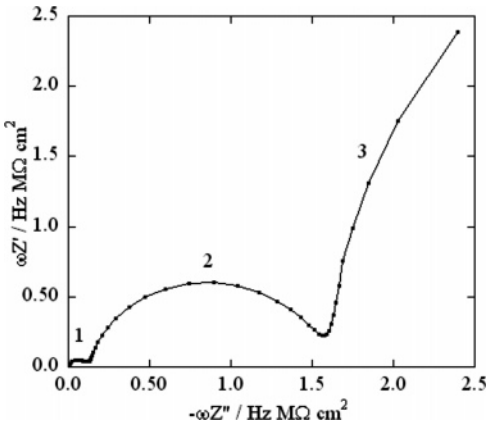

Figure 4. Plot of $\omega Z'$ versus $\omega Z''$ at a tBLM incorporating gramicidin from its 1.0×10^{-7} M solution in aqueous 0.1 M KCl recorded at -0.525 V.

fused semicircles, denoted by numbers from 1 to 3, are clearly visible. In a $\omega Z'$ versus $\omega Z''$ plot, a semicircle corresponds to a *RC* mesh;[28] the diameter of the semicircle measures the reciprocal, $1/C$, of the capacity of the *RC* mesh, while the ω value at the maximum of the semicircle measures the reciprocal of its time constant, $\tau = RC$. The frequency increases in the direction of increasing $\omega Z''$. Therefore, the time constants of the *RC* meshes in Figure 4 decrease as we proceed along the $\omega Z''$ axis. This behavior is similar to that observed with an identical tBLM incorporating the ion carrier valinomycin, under otherwise identical conditions.[28] By following the gradual evolution of semicircles 1 and 2 by varying the applied potential *E*, the corresponding values of the capacity and conductance were determined as a function of *E*.

Figures 5−7 show plots of these quantities against *E*, upon subtracting the corresponding quantities in the absence of gramicidin. Therefore, these curves exclusively express the contribution to these quantities from the progressive flow of potassium ions into the tBLM with a negative shift in the applied potential. The quantities in these figures have an overbar to distinguish them from the capacities and conductances obtained in the absence of gramicidin. Both the capacity $\bar{C}_2$ and the conductance $\bar{g}_2 \equiv 1/\bar{R}_2$ of mesh 2 tend to a maximum in the proximity of -1.0 V, while those, $\bar{C}_1$ and $\bar{g}_1 \equiv 1/\bar{R}_1$, of mesh 1 show maxima at about -0.60 V.

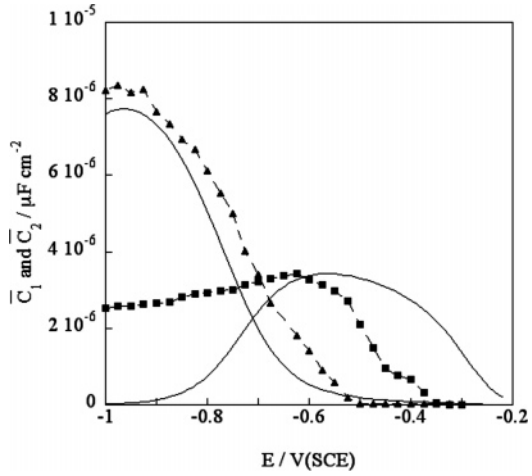

Figure 5. Plots of $\bar{C}_2$(solid triangles) and $\bar{C}_1$ (solid squares) against *E* at a tBLM incorporating gramicidin from its 1.0×10^{-7} M solution in aqueous 0.1 M KCl. The corresponding solid curves are the fits obtained for $K_1 = 5 \times 10^{-3}$ and $K_2 = 3 \times 10^5$ cm^3 mol^{-1}, $C_0 = 4$, $C_1 = 7$, and $C_2 = 1$ μF cm^{-2}, $\chi_1 = -0.250$ V, and $\Gamma_m = 1 \times 10^{-11}$ mol cm^{-2}. The increase in gramicidin dimer formation with an increase in conductivity was accounted for as described in the text.

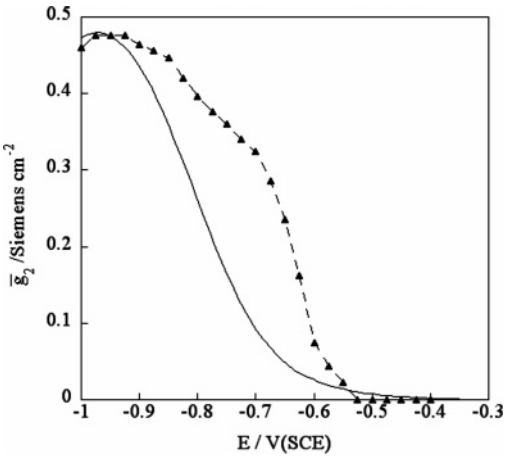

Figure 6. Plot of $\bar{g}_2$(solid triangles) against *E* at a tBLM incorporating gramicidin from its 1.0×10^{-7} M solution in aqueous 0.1 M KCl. The solid curve is the fit obtained for the same equilibrium parameters as those in Figure 5 and for $\alpha = 0.5$, $k_{1,f} = 2.25 \times 10^{13}$ cm^2 s^{-1} mol^{-1}, and $k_{2,f} = 2.2 \times 10^9$ cm^3 s^{-1} mol^{-1}. The increase in gramicidin dimer formation with an increase in conductivity was accounted for as described in the text.

In the Discussion section, it will be shown that $\bar{C}_2$, $\bar{g}_2$ and $\bar{C}_1$, $\bar{g}_1$ are to be ascribed to the movement of K^+ ions across the lipid bilayer moiety and across the TEO moiety, respectively. For comparison, in Figure 7, the $\bar{g}_1$versus *E* plot for gramicidin is reported together with the corresponding plot for valinomycin, as obtained in ref 28 by incorporating valinomycin from its 1.5×10^{-7} M solution in aqueous 0.1M KCl in an identical tBLM. In analogy with the behavior of a tBLM incorporating valinomycin,[28] the large semicircle 3 in Figure 4, which is independent of the applied potential, is due to the aqueous solution adjacent to the tBLM; it will not be considered further.

Discussion

Let us denote the dipole moment of the gramicidin molecule by μ, the transmembrane potential by ϕ_2, and the corresponding electric field by $-\phi_2/d$, where *d* is the thickness of the hydrocarbon tail region of the lipid bilayer. The ratio of the number density, N', of the gramicidin dipoles aligned in the

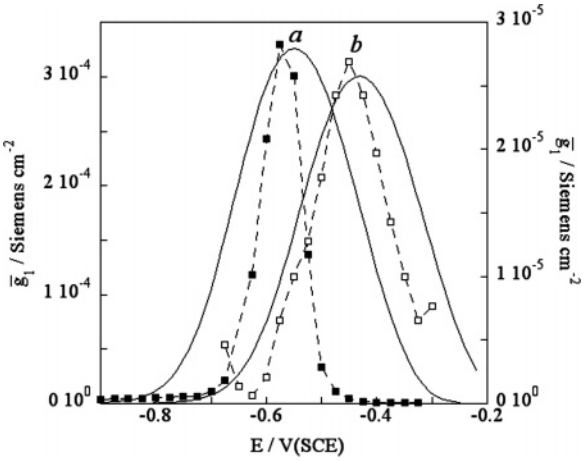

Figure 7. Curve a is a plot of the conductance $\bar{g}_1$ against E at a tBLM incorporating gramicidin from its 1.0×10^{-7} M solution in aqueous 0.1 M KCl. The solid squares are experimental values, while the solid curve was calculated from the model for the same values as those in Figures 5 and 6. The increase in gramicidin dimer formation with an increase in conductivity was accounted for as described in the text. Curve b is an analogous plot obtained at a tBLM incorporating 1.5×10^{-7} M valinomycin under otherwise identical conditions. Open squares are experimental values, while the solid curve was calculated for the same equilibrium parameters as those in Figure 5 and for $\alpha = 0.5$, $k_{1,f} = 2 \times 10^{12}$ cm^2 s^{-1} mol^{-1}, and $k_{2,f} = 4.5 \times 10^6$ cm^3 s^{-1} mol^{-1}. The left-hand axis refers to curve a and the right-hand one to curve b.

direction of increasing ϕ_2 to that, N'', of the dipoles aligned in the opposite direction is, therefore, given by

$$N'/N'' = \exp(2\mu\phi_2/dkT) \tag{1}$$

where ϕ_2 is negative. Denoting by N and N_2 the number densities of all gramicidin molecules and of the dimeric ion channels, respectively, we have

$$N = N' + N'' + 2N_2 \tag{2}$$

Let k_a and k_d denote the association and dissociation rate constants for dimer formation. The rate of change of N_2 is given by

$$dN_2/dt = k_a N' N'' - k_d N_2 \tag{3}$$

Combining eqs 1−3 and denoting the fraction, N_2/N, of dimers by y, we obtain

$$dy/dt = k'_a (1 - 2y)^2 - k_d y \tag{4}$$

with

$$k'_a \equiv k_a N e^{\beta\phi_2}/(e^{\beta\phi_2} + 1)^2 \quad \beta \equiv 2\mu/dkT \tag{5}$$

When the current I following a potential step attains stationary conditions, dy/dt equals zero, and y is given by

$$y_\infty = 1/2 + (k_d - \sqrt{k_d^2 + 8k'_a k_d})/(8k'_a) \tag{6}$$

It is evident that the potential-dependent association rate constant k'_a expressed by eq 5 decreases with an increase in $|\phi_2|$, causing the stationary current I to increase with $|\phi_2|$ less than linearly. This prediction contrasts with the experimental behavior in Figure 3, where I increases with ϕ_d more than linearly.

To account for the experimental behavior, it is assumed that the increase of k'_a with $|\phi_2|$ is due to the dimeric gramicidin channels being stabilized by the single-file ionic flux along them. In other words, the increase in k'_a is related to the increase in the ionic flux and, hence, in the ionic current I. To fit eqs 5 and 6 to the experimental plots in Figure 3 on the basis of this assumption, the following "feedback" procedure was adopted. In the case of Ohmic behavior, the stationary current is proportional to the product of the fraction, y_∞, of channels by $|\phi_2|$. The absolute value, $|\phi_2|$, of the transmembrane potential is increased progressively by 1 mV steps, and at each step, k'_a is multiplied by the quantity $y_\infty|\phi_2|$, which is taken as a measure of the ionic flux and is treated as dimensionless. The difference between the value of the quantity $(y_\infty|\phi_2|\ k'_a)$ at any given jth step and its value at the $(j-1)$th step is then divided by a suitable "damping factor", df. The value ascribed to the "actual" association rate constant at the jth step is then given by $k''_a = (y_\infty|\phi_2|k'_a)_{j-1} + [(y_\infty|\phi_2|k'_a)_j - (y_\infty|\phi_2|k'_a)_{j-1}]/df$. This iterative procedure starts at the second step, with the association rate constant at the first step being set equal to k'_a. The damping factor serves to moderate the increase of the association rate constant with the increase in ion flux. To fit the I versus ϕ_2 plots in Figure 3, the potential-independent dissociation rate constant k_d was set equal to the value 1.6 s^{-1} determined by Bamberg and Läuger on BLMs,[24] and d was set equal to 30 Å. The best fit to the experimental plots in Figure 3 was obtained by setting the gramicidin dipole moment μ equal to 9 Debye. This value is somewhat higher than that, ∼4 Debye, estimated by Urry[14] from the C−O bond moments of the conducting $\beta^6_{3.3}$-helix. However, the dipole moment of the whole peptide molecule may be higher due to the side chains of the amino acid residues. Thus, for instance, the dipole moments, ∼2 Debye, of the four Trp residues have a positive component in the direction from the C- to the N-terminus in the right-handed structure of the helix.[35] The dashed curve in Figure 3 is the calculated plot of $(y_\infty|\phi_2|)$ versus ϕ_2 that provides the best fit to the two experimental plots. It was obtained by setting k'_a at $\phi_2 = 0$ equal to 0.1 s^{-1} and the damping factor df equal to 50 and by then normalizing the vertical axis of the calculated curve to those of the corresponding experimental plots. The inset of Figure 3 shows the calculated value of the actual association rate constant k''_a against ϕ_2. For $|\phi_2| < 100$ mV, this quantity is low and almost independent of ϕ_2 due to the compensation between the decrease in the $\exp(\beta\phi_2)/[1 + \exp(\beta\phi_2)]^2$ factor and the increase in current. Then, at higher $|\phi_2|$ values, the last contribution prevails, and k''_a increases rapidly. Extrapolation to $\phi_2 = 0$ yields a k''_a value of 0.037 s^{-1}, which, once divided by k_d=1.6 s^{-1}, yields a value of 0.023 for $k''_a/k_d = K_d N/4$, where K_d is the equilibrium constant for dimer formation at $\phi_2 = 0$. The latter equation accounts for the fact that k''_a embodies the quantity $N \exp(\beta\phi_2)/[1 + \exp(\beta\phi_2)]^2$, which is not included in K_d and equals $N/4$ at $\phi_2 = 0$. At zero transmembrane potential, we also have $N' = N'' = N_1/2$, where N_1 is the total number density of the gramicidin monomers. Consequently, at $\phi_2 = 0$, we can write $K_d = 4N_2/N_1^2$ and $N = 2N_2 + N_1$. Combining the two latter equations and setting $K_d N/4 = 0.023$, we obtain a N_1/N ratio equal to 0.96. This implies that at $\phi_2 = 0$, when no ionic flux along the gramicidin channel takes place, gramicidin is present almost exclusively in the monomeric form. In other words, it is the single-file ionic flux along the gramicidin dimers that stabilizes them.

That the gramicidin dimer-to-monomer ratio is very low in the absence of ionic flux and increases notably with an increase in the latter is also apparent from a comparison of the impedance spectra of a tBLM incorporating gramicidin with those of an identical tBLM incorporating the ion carrier valinomycin. Both gramicidin and valinomycin have a high selectivity for the

monovalent cation K^+. Figure 7 shows that the $\bar{g}_1$ versus E plot for the TEO moiety is shifted by more than 100 mV toward more negative potentials when passing from valinomycin to gramicidin. This points to a more sluggish increase in conductivity by gramicidin than by valinomycin, as K^+ ions start to be attracted into the TEO moiety by a negative shift in the applied potential. Nonetheless, $\bar{g}_1$ attains a maximum value that is 1 order of magnitude higher with gramicidin than that with valinomycin, in agreement with the higher turnover rate expected for a channel with respect to an ion carrier. The driving force that moves K^+ ions into the TEO moiety across the lipid bilayer at a given applied potential E is necessarily the same in the same tBLM, independent of the incorporation of valinomycin or gramicidin. Consequently, gramicidin is scarcely active in conducting K^+ ions at potentials at which valinomycin is already very active in complexing K^+ ions and shuttling them across the lipid bilayer moiety. This points to a low percentage of gramicidin conducting dimers at these potentials.

A detailed analysis of the impedance spectra of tBLMs incorporating gramicidin from aqueous 0.1 M KCl was carried out by using an approach analogous to that adopted for the incorporation of valinomycin,[28] OmpF porin,[29] and melittin[30] in the same tBLM. According to this approach, the whole electrified interface is regarded as consisting of four substructures with different dielectric properties, namely, the lipoic acid residue, the TEO hydrophilic spacer, the lipid bilayer moiety, and the aqueous solution adjacent to the tBLM. The interphase is represented by an equivalent circuit consisting of four *RC* meshes in series, one per each substructural element. The elements of this equivalent circuit represent ideal lumped-constant properties, even though the K^+ ions are distributed in space across the tBLM. This general approach[28] assumes that the charges within the tBLM are located as shown in Figure 1: a free electronic charge density q on the surface of the mercury electrode, a charge density $F\Gamma_1$ at the boundary between the lipoic acid residue and the TEO moiety, and a charge density $F\Gamma_2$ at the boundary between the TEO moiety and the lipid bilayer moiety. Here, Γ_1 and Γ_2 are surface concentrations of K^+.

The potential difference ϕ_t across the whole tBLM due to this charge distribution is expressed by the equation

$$\phi_t = \frac{q}{C_0} + \left[\frac{q + F\Gamma_1}{C_1} + \chi_1\right] + \left[\frac{q + F(\Gamma_1 + \Gamma_2)}{C_2}\right] \equiv \phi_0 + \phi_1 + \phi_2 \quad (7)$$

In this equation, C_0, C_1, and C_2 are, in the order, the "intrinsic" capacities of the lipoic acid residue, the hydrophilic spacer, and the lipid bilayer moiety, as measured in the absence of ionophores, while ϕ_0, ϕ_1, and ϕ_2 are the potential differences across these dielectric slabs. ϕ_1 includes the dipole potential, χ_1, of the hydrophilic spacer, which was estimated at about -0.250 V, negative toward the metal, on the basis of independent measurements.[34] The extrathermodynamic absolute potential difference ϕ_t across the whole mercury|(aqueous solution) interphase is more positive than the potential E measured versus a SCE by about 0.250 V[33]. Therefore, ϕ_t can be directly related to the applied potential E.

The incorporation of a channel-forming peptide or protein alters the conductance and capacity of the substructural elements with respect to their "intrinsic" values by an amount denoted by an overbar. Roughly speaking, the alteration, $\bar{g}_i$, in the conductance of any given substructural element i is set equal to the rate of change with E of the current that flows to and fro along the element, while the alteration, $\bar{C}_i$, in its capacity is set equal to the rate of change with E of the charge that accumulates at the boundary of the element, on its metal side. To this end, the current, j_2, which flows along the lipid bilayer moiety, is expressed by a Butler−Volmer-like equation.[28] The forward and backward rate constants for the surmounting of the potential energy barrier associated with the lipid bilayer moiety are denoted by $k_{2,f}$ and $k_{2,b}$ when ϕ_2 equals zero. Under equilibrium conditions (that is, for $j_2 = 0$), this equation reduces to a Langmuir isotherm, with a potential-independent adsorption equilibrium constant, $K_2 = k_{2,f}/k_{2,b}$. An analogous expression is used for the current, j_1, flowing along the TEO hydrophilic spacer. The forward and backward rate constants for the surmounting of the potential energy barrier associated to the TEO moiety are denoted by $k_{1,f}$ and $k_{1,b}$ when ϕ_1 equals zero, and the corresponding adsorption equilibrium constant is given by $K_1 = k_{1,f}/k_{1,b}$. The procedure adopted to fit the equivalent circuit to the experimental data is outlined in the Supporting Information. The same equilibrium parameters providing the best fit to the impedance spectra of tBLMs incorporating valinomycin were adopted for the fitting, while the kinetic parameters $k_{1,f}$ and $k_{2,f}$ were increased with respect to those used for valinomycin to account for the notable increase in the maximum values of $\bar{g}_1$ and $\bar{g}_2$ when passing from valinomycin to gramicidin. Thus, the following parameters were employed: $C_0 = 4$, $C_1 = 7$, and $C_2 = 1$ μF cm^{-1}; $\chi_1 = -0.250$ V; $K_1 = 5 \times 10^{-3}$, $K_2 = 3 \times 10^5$ cm^3 mol^{-1}; and $k_{1,f} = 2.25 \times 10^{13}$ cm^2 s^{-1} mol^{-1}, and $k_{2,f} = 2.2 \times 10^9$ cm^3 s^{-1} mol^{-1}.

To relate the increase in gramicidin dimers to the increase in the conductivity $\bar{g}_2$ across the lipid bilayer, a feedback procedure analogous to that previously used for the stationary current measurements was adopted. Thus, capacities and conductances were calculated starting from an applied potential $E = -0.200$ V, where no K^+ flux occurs due to the unfavorable electric field. The potential E was then progressively decreased by -10 mV steps, and, at each step the fraction, $y_\infty = N_2/N$, of dimers was estimated by the procedure already described, with the same k'_a, k_d and df values used for the dashed curve in Figure 3, namely, $k'_a = 0.1$ s^{-1}, k_d=1.6 s^{-1}, and df = 50; the only difference consisted in multiplying k'_a by $\bar{g}_2$, normalized to its maximum value attained at -1.00 V, rather than by $y_\infty|\phi_2|$. The adsorption equilibrium constant, K_2, and the forward rate constant, $k_{2,f}$ relative to K^+ movement across the lipid bilayer were assumed to increase proportionally to the number density, y_∞, of dimers. The maximum value attainable by y_∞ is 0.5. At each step, K_2 and k_{2f} were, thus, multiplied by the quantity $2y_\infty$, so as to give K_2 the possibility of attaining the value that provides the best fit to the impedance spectra of a tBLM incorporating valinomycin.[28] In principle, the equilibrium constant K_2 for ion translocation across the lipid bilayer moiety should not depend on the nature of the incorporated ionophore but only on the two phases separated by the bilayer. In practice, however, true equilibrium conditions are not attained even at the lowest frequencies adopted in the present ac measurements. Consequently, K_2 should be regarded as a "pseudo-equilibrium" constant.

The fact that the quantities $\bar{C}_1$ and $\bar{g}_1$, relative to the TEO moiety, attain a maximum at less negative potentials than the quantities $\bar{C}_2$ and $\bar{g}_2$, relative to the lipid bilayer moiety, is due to the negative dipole potential, χ_1, located in the TEO moiety, which favors an incipient accumulation of K^+ ions on the metal side of this hydrophilic spacer as the potential is progressively shifted in the negative direction. On the other hand, the height of the potential energy barrier due to the lipid bilayer decreasing

toward more negative potentials causes the conductance $\bar{g}_2$, which is responsible for the accumulation of K^+ on the solution side of the TEO moiety, to become ultimately much greater than $\bar{g}_1$.

The solid curves in Figures 5−7 are fits of the above equivalent circuit to the experimental plots of $\bar{C}_1$, $\bar{C}_2$, $\bar{g}_2$, and $\bar{g}_1$ against E, calculated as described in the Supporting Information, using the parameters reported in the legends. Agreement is only semiquantitative. The solid curve b in Figure 7 is the fit to the experimental $\bar{g}_1$ versus E plot for valinomycin, calculated using the same equivalent circuit and the same equilibrium parameters as those for gramicidin. Only the kinetic parameter $k_{1,f}$ was decreased from 2.25×10^{13} to 2×10^{12} cm^2 s^{-1} mol^{-1} to account for the lower conductivity $\bar{g}_1$ of valinomycin. It should be noted that the negative shift in the calculated solid curves of Figure 7, in passing from valinomycin to gramicidin, is only determined by the feedback procedure used to relate the gramicidin dimer formation to the conductivity, $\bar{g}_2$, across the lipid bilayer moiety.

In conclusion, potentiostatic current and charge versus time curves as well as impedance spectroscopy measurements indicate that gramicidin monomers incorporated in a lipid bilayer have a low tendency to form conducting dimers in the absence of ionic flux; dimer formation is notably increased by single-file movement of monovalent cations along the dimeric channels.

Acknowledgment. Thanks are due to Ente Cassa di Risparmio di Firenze for financial support through the PROMELAB project.

Supporting Information Available: The approach that applies the concepts of electrochemical impedance spectroscopy to a model of the electrified interphase and to the kinetics of potassium ion transport across the tBLM. This material is available free of charge via the Internet at http://pubs.acs.org.

References and Notes

(1) Veatch, W. R.; Fossel, E. T.; Blout, E. R. *Biochemistry* **1974**, *13*, 5249−5256.
(2) Veatch, W. R.; Blout, E. R. *Biochemistry* **1974**, *13*, 5257−5264.
(3) Bystrov, V. F.; Arseniev, A. S. *Tetrahedron* **1988**, *44*, 925−940.
(4) Bañó, M. C.; Braco, L.; Abad, C. *J. Chromatogr*. **1988**, *458*, 105−116.
(5) Abdul-Manan, N.; Hinton, J. F. *Biochemistry* **1994**, *33*, 6773−6783.
(6) Xu, F.; Wang, A.; Vaughn, J. B.; Cross, T. A. *J. Am. Chem. Soc.* **1996**, *118*, 9176−9177.
(7) LoGrasso, P. V.; Moll, F., III; Cross, T. A. *Biophys. J*. **1988**, *54*, 259−267.
(8) Bañó, M. C.; Braco, L.; Abad, C. *FEBS Lett.* **1989**, *250*, 67−71.
(9) O'Cornell, A. M.; Koeppe, R. E., II; Andersen, O. S. *Science* **1990**, *250*, 1256−1259.
(10) Bañó, M. C.; Braco, L.; Abad, C. *Biochemistry* **1991**, *30*, 886−894.
(11) Bañó, M. C.; Braco, L.; Abad, C. *Biophys. J.* **1992**, *63*, 70−77.
(12) Greathouse, D. V.; Hinton, J. F.; Kim, K. S.; Koeppe, R. E., II. *Biochemistry* **1994**, *33*, 4291−4299.
(13) Hurry, D. W. *Proc. Natl. Acad. Sci. U.S.A.* **1971**, *68*, 672−676.
(14) Hurry, D. W. *Proc. Natl. Acad. Sci. U.S.A.* **1972**, *69*, 1610−1614.
(15) Bamberg, E.; Apell, H.-J.; Alpes, H. *Proc. Natl. Acad. Sci. U.S.A.* **1977**, *74*, 2402−2406.
(16) Apell, H.-J.; Bamberg, E.; Alpes, H.; Läuger, P. *J. Membr. Biol*. **1977**, *31*, 171−188.
(17) Weinstein, S.; Wallace, B. A.; Blout, E. R.; Morrow, J. S.; Veatch, W. *Proc. Natl. Acad. Sci. U.S.A.* **1979**, *76*, 4230−4234.
(18) Hurry, D. W.; Prasad, K. U.; Trapane, T. L. *Proc. Natl. Acad. Sci. U.S.A.* **1982**, *79*, 390−394.
(19) Salom, D.; Bañó, M. C.; Braco, L.; Abad, C. *Biochem. Biophys. Res. Commun.* **1995**, *209*, 466−473.
(20) Cotton, M.; Xu, F.; Cross, T. A. *Biophys. J.* **1997**, *73*, 614−623.
(21) Salom, D.; Pérez-Payá, E.; Pascal, J.; Abad, C. *Biochemistry* **1998**, *37*, 14279−14291.
(22) Zhang, Z.; Pascal, S. M.; Cross, T. A. *Biochemistry* **1992**, *31*, 8822−8828.
(23) Arumugan, S.; Pascal, S.; North, C. L.; Hu, W.; Lee, C.; Cotten, M.; Ketchem, R. R.; Xu, F.; Brenneman, M.; Kovacs, F.; Tian, F.; Wang, A.; Huo, S.; Cross, T. A. *Proc. Natl. Acad. Sci. U.S.A.* **1996**, *93*, 5872−5876.
(24) Bamberg, E.; Läuger, P. *J. Membr. Biol*. **1973**, *11*, 177−194.
(25) Bamberg, E.; Benz, R. *Biochim. Biophys. Acta* **1976**, *426*, 570−580.
(26) Schiller, S. M.; Naumann, R.; Lovejoy, K.; Kunz, H.; Knoll, W. *Angew. Chem., Int. Ed.* **2003**, *42*, 208−211.
(27) Naumann, R.; Schiller, S. M.; Giess, F.; Grohe, B.; Hartman, K. B.; Kärcher, I.; Köper, I.; Lübben, J.; Vasilev, K.; Knoll, W. *Langmuir* **2003**, *19*, 5435−5443.
(28) Becucci, L.; Moncelli, M. R.; Naumann, R.; Guidelli, R. *J. Am. Chem. Soc*. **2005**, *127*, 13316−13323.
(29) Becucci, L.; Moncelli, M. R.; Guidelli, R. *Langmuir* **2006**, *22*, 1341−1346.
(30) Becucci, L.; Romero Léon, R.; Moncelli, M. R.; Rovero, P.; Guidelli, R. *Langmuir* **2006**, *22*, 6644−6650.
(31) Moncelli, M. R.; Becucci, L. *J. Electroanal. Chem*. **1997**, *433*, 91−96.
(32) Tadini Buoninsegni, F.; Herrero, R.; Moncelli, M. R. *J. Electroanal. Chem*. **1998**, *452*, 33−42.
(33) Becucci, L.; Moncelli, M. R.; Guidelli, R. *Langmuir* **2003**, *19*, 3386−3392.
(34) Moncelli, M. R.; Becucci, L.; Schiller, S. M. *Bioelectrochemistry* **2004**, *63*, 161−167.
(35) Hurry, D. W.; Luan, C.-H. In *Bioelectrochemistry of Biomacromolecules*; Lenaz G., Milazzo, G., Eds.; Birkhäuser Verlag: Basel, Switzerland, 1997; p 118.